Thermochimica Acta, 191 (1991) 341–351
Elsevier Science Publishers B.V., Amsterdam

Measurements of enthalpies of phase transition for chromium Chevrel-phase sulphides in the temperature range from 400 to 900 K

Akihiro Oshima, Eitaroh Ike, Hirofumi Hinode and Masataka Wakihara

Department of Chemical Engineering, Tokyo Institute of Technology, Ookayama, Meguro-ku, Tokyo 152 (Japan)

(Received 3 April 1991)

Abstract

Measurements of the enthalpy increment, $H_T - H_{298}$, were carried out for chromium Chevrel-phase sulphides (CMS), $Cr_xMo_6S_{8-y}$ ($1.4 \leqslant x \leqslant 2.0$, $7.5 \leqslant 8 - y \leqslant 8.0$), in the temperature range from 400 to 900 K by the drop method using a high-temperature Calvet-type twin calorimeter. We obtained the molar enthalpies and temperatures for the phase transition from a triclinic (low-temperature phase) to a rhombohedral structure (high-temperature phase), as well as the heat capacities of CMSs with twelve different compositions. These are the first experimental results yielding thermodynamic information for CMS.

INTRODUCTION

The ternary molybdenum chalcogenides, $M_xMo_6X_{8-y}$ (M = Ag, Pb, Sn, Ni, Cu, etc. X = S, Se, Te), generally called Chevrel-phase compounds, are of special interest due to their high superconducting critical temperatures [1] and the pressure-dependence of their transition temperatures [2]. Sulphides of such type containing several building blocks with the formula Mo_6S_8, generally crystallise in rhombohedral (or hexagonal) structures [3]. However, some of these sulphides with a small M cation, e.g. Fe or Cu, usually exhibit a triclinic deformation, depending on the temperature and content of metal and sulphur. Several studies concerning the structural phase transition have been reported [4,5], but none of them has studied the thermodynamic properties of these compounds, except for the specific heat capacity measurement at extremely low temperatures.

Recently, our research group has determined the single-phase field and phase relations of $Cr_xMo_6S_{8-y}$ at 1000 °C (Fig. 1). The presence of the ternary phase compounds, triclinic $Cr_xMo_6S_{8-y}$, was confirmed by X-ray powder diffractometry of the quenched samples. The single-phase field of triclinic chromium Chevrel-phase sulphides is denoted by open circles in this diagram. In the isothermal section at 1000 °C, the chromium content,

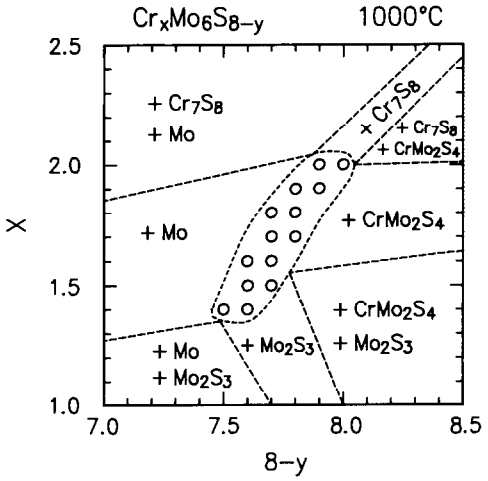

Fig. 1. Single phase region of $Cr_xMo_6S_{8-y}$ at 1000 °C.

x, and the sulphur content, $(8-y)$, in $Cr_xMo_6S_{8-y}$ vary between $1.4 \leqslant x \leqslant 2.0$ and $7.5 \leqslant 8-y \leqslant 8.0$, respectively, while the chromium content increases with increasing sulphur content. These samples were analysed by high-temperature X-ray powder diffractometry (Cu Kα radiation) at ambient pressure.

In this paper, we show that each compound of different composition can transform from a triclinic distorted structure to a rhombohedral structure above room temperature. The enthalpies and temperatures of the phase transition as well as the heat capacities of CMS measured by the drop method using a Calvet-type calorimeter, were found to depend on their chromium and sulphur compositions.

EXPERIMENTAL

Sample preparation

The starting materials were prepared from molybdenum (99.9%, Wako Pure Chemical Industries Ltd.), reagent grade sulphur (99.9999%, Wako Pure Chemical Industries Ltd.) and CrS_x, which was synthesised previously using the following method. Chromium powder (99.9%, Soekawa Chemical Co., Ltd.) was sulphurised in a furnace at 800 °C by passage of hydrogen sulphide gas through the furnace for 48 hours. The powder thus formed was ground and placed in the furnace at 800 °C for another 48 hours. The prepared sample was identified using the X-ray powder diffraction method. The chemical composition of CrS_x was determined as $x = 1.485$ by complete oxidation of the samples to Cr_2O_3 in air at 900 °C for 48 hours. The $Cr_xMo_6S_{8-y}$ samples were prepared by mixing $CrS_{1.485}$, Mo and S in the

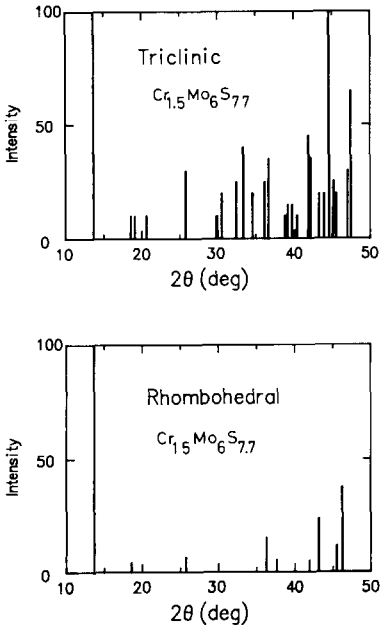

Fig. 2. Typical X-ray diffraction patterns of CMS.

desired ratio to an accuracy of 0.01 mg. The mixture was heated in a vacuum-sealed ampoule at 1000 °C for 12 hours, followed by quenching. After grinding, the sample was sealed again under vacuum and heated at 1000 °C for 72 hours followed by quenching. The phase identification and estimation of lattice parameters for the quenched samples were performed by powder X-ray diffractometry with nickel-filtered Cu Kα radiation. The phase transitions of these samples from a triclinic room-temperature phase to a rhombohedral high-temperature phase were confirmed by high-temperature X-ray powder diffractometry. Typical X-ray powder patterns are shown in Fig. 2.

Apparatus and procedure

The Calvet-type twin calorimeter designed for operation at temperatures up to 650 °C [6,7] was used for the drop calorimetry of CMS compounds.

TABLE 1

Conditions for the experiment on Cr Chevrel-phase sulphides

Temperature of calorimeter	400–900 K
Particle size of sample	102–169 μm
Amount of sample	30– 40 mg
Weight of quartz ampoule	90–120 mg

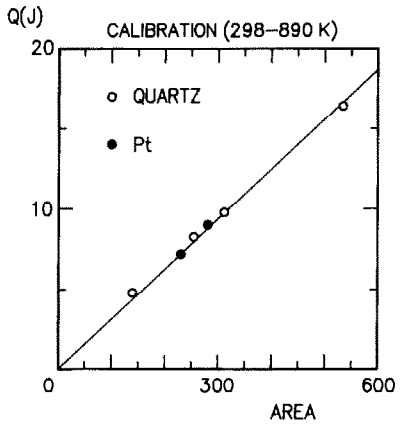

Fig. 3. Calibration of the calorimeter at 890 K using quartz and Pt.

In this calorimeter the thermal effect was detected as electrical output with a thermocouple. The electrical signal was amplified by a microvolt amplifier and was integrated to obtain the enthalpy change using an on-line computer. Each sample, about 35 mg with different compositions, was sealed under vacuum in a quartz ampoule. This ampoule, at room temperature ($25 \pm 1°$ C), was placed in a calorimeter the temperature of which was kept constant above room temperature. The temperature of the calorimeter was changed from 400 to 900 K in order to measure the variation in the $H_T - H_{298K}$ values with temperature. The optimum experimental conditions determined for the present study are summarised in Table 1.

Calibration of the calorimeter was performed by measuring the enthalpy increment, $H_T - H_{298K}$, of quartz and platinum [8] at several temperatures.

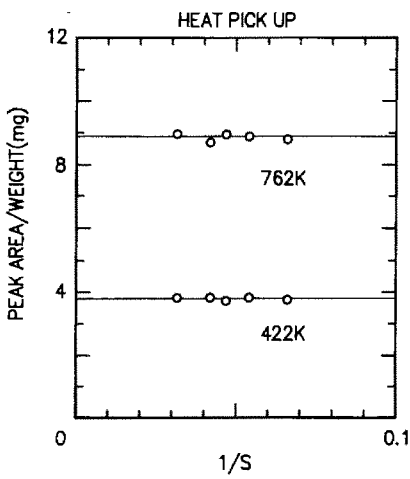

Fig. 4. Relation between calibration factor and surface area of quartz.

Figure 3 shows the results of all the calibrations. In order to correct our measurements for the slight pick-up of heat caused by radiative heat transfer to the sample during its transfer from room temperature into the calorimeter, calibration measurements were made by dropping quartz rods with different surface areas into the calorimeter. The results are presented in graphical form in Fig. 4, where the calibration constants (peak area/mg quartz) were plotted against the inverse surface area (S^{-1}). The straight lines in Fig. 4 were obtained by a least-squares method from the plotted data. The value obtained by extrapolating S^{-1} to zero was regarded as the true calibration constant. As the gradients of the lines at both low temperature and high temperature were almost zero, it was unnecessary to correct our enthalpy increment data.

RESULTS AND DISCUSSION

Enthalpy increment

The enthalpy increments $H_T - H_{298K}$ for twelve compositions of $Cr_xMo_6S_{8-y}$ obtained in the present study are given in Table 2. The results of two different compositions are plotted graphically in Fig. 5a and 5b. It can be seen from the plots of temperature versus $H_T - H_{298K}$ in Fig. 5 that there is a discontinuity indicating the first-order transition of $Cr_{1.4}Mo_6S_{7.5}$ and $Cr_{1.8}Mo_6S_{7.7}$. Other samples with different compositions showed the same discontinuity, except for the three compositions, $Cr_{1.9}Mo_6S_{7.8}$, $Cr_{1.9}Mo_6S_{7.9}$ and $Cr_{2.0}Mo_6S_{8.0}$. We believe that these samples also exhibit a phase transition but because we could not raise the temperature of our calorimeter above 900 K, the phase transition of these three samples could not be observed. However, they are expected to exhibit a phase transition at higher temperatures.

The enthalpy increments for $Cr_xMo_6S_{8-y}$ were fitted to a linear function of temperatures before and after the phase transition by the least-squares method. The differentiation of these equations with respect to temperature yields the molar heat capacity. The temperature of the phase transition was determined from the mean value of the adjacent temperatures at which the discontinuity occurred, and the enthalpy of phase transition was estimated by substituting the temperatures of phase transition into the fitted equations for each composition. The values estimated in this way are summarised in Table 3.

Temperature of phase transition

The results for the temperatures of the phase transition from a triclinic to a rhombohedral structure are plotted graphically in Fig. 6. As can be seen from Fig. 6, the temperature of the phase transition of CMS increases

TABLE 2
Dependence of enthalpy increment on temperature for $Cr_xMo_6S_{8-y}$

T (K)	$\Delta^T_{298K} H_m$ (kJ mol^{-1})	T (K)	$\Delta^T_{298K} H_m$ (kJ mol^{-1})
$Cr_{1.4}Mo_6S_{7.5}$			
298	0	phase transition	
393	40.1 ± 1.5	467	87.1 ± 1.1
400	42.2 ± 4.5	530	109.8 ± 4.3
410	44.9 ± 2.2	607	141.3 ± 2.2
435	55.5 ± 0.9	682	171.2 ± 2.3
440	57.2 ± 3.4	747	191.6 ± 6.8
448	59.2 ± 0.8	821	218.5 ± 1.3
$Cr_{1.4}Mo_6S_{7.6}$			
298	0	phase transition	
400	38.6 ± 1.0	538	122.6 ± 1.7
422	43.5 ± 2.2	585	135.4 ± 1.5
479	65.0 ± 2.1	649	165.4 ± 1.5
496	73.1 ± 2.1	706	184.9 ± 0.7
524	83.1 ± 2.6	826	231.4 ± 2.6
$Cr_{1.5}Mo_6S_{7.6}$			
298	0	phase transition	
422	52.9 ± 1.5	620	169.6 ± 3.1
473	72.6 ± 0.7	649	181.7 ± 4.8
524	94.3 ± 1.8	706	201.3 ± 4.8
585	112.1 ± 5.9	826	247.6 ± 7.0
602	124.4 ± 1.4		
$Cr_{1.5}Mo_6S_{7.7}$			
298	0	phase transition	
422	51.6 ± 0.9	659	184.7 ± 4.1
473	69.7 ± 3.1	668	188.2 ± 2.3
524	88.7 ± 3.4	706	201.7 ± 2.2
585	113.0 ± 2.9	771	233.0 ± 4.3
649	140.8 ± 6.0	826	251.0 ± 10.0
$Cr_{1.6}Mo_6S_{7.6}$			
298	0	phase transition	
400	40.7 ± 1.5	633	183.0 ± 4.9
422	52.4 ± 1.5	649	187.0 ± 1.3
473	70.2 ± 2.7	706	212.4 ± 6.3
496	85.2 ± 1.3	797	248.4 ± 2.2
524	91.9 ± 1.3	826	258.0 ± 3.4
585	113.0 ± 2.1	851	267.6 ± 1.5
620	129.9 ± 5.4		
$Cr_{1.6}Mo_6S_{7.7}$			
298	0	659	147.8 ± 2.8
422	52.8 ± 1.6	phase transition	
473	72.5 ± 3.7	668	199.4 ± 1.7
524	91.2 ± 1.9	706	211.3 ± 3.2
585	115.0 ± 2.3	740	226.8 ± 4.8
649	145.1 ± 1.3	826	262.4 ± 3.3

TABLE 2 (continued)

T (K)	Δ^{T}_{298K} H_m (kJ mol^{-1})	T (K)	Δ^{T}_{298k} H_m (kJ mol^{-1})
$Cr_{1.7}Mo_6S_{7.7}$			
298	0	phase transition	
410	55.3 ± 1.2	747	242.8 ± 4.9
435	65.7 ± 4.5	759	249.4 ± 5.4
467	76.4 ± 3.2	788	258.4 ± 6.3
530	101.6 ± 1.7	821	277.9 ± 3.2
607	133.6 ± 1.6	839	283.2 ± 4.0
682	166.9 ± 3.6	888	300.5 ± 5.2
724	185.7 ± 8.1		
$Cr_{1.8}Mo_6S_{7.7}$			
298	0	683	163.3 ± 1.6
400	49.7 ± 0.9	740	188.6 ± 3.7
422	54.7 ± 2.1	phase transition	
473	76.0 ± 3.0	758	247.8 ± 2.2
496	89.9 ± 0.3	771	250.8 ± 3.8
524	96.3 ± 3.9	797	261.4 ± 1.2
585	124.6 ± 2.0	826	272.6 ± 4.9
649	148.4 ± 4.3	851	286.5 ± 1.0
668	160.7 ± 5.8	888	300.8 ± 5.4
$Cr_{1.8}Mo_6S_{7.8}$			
298	0	phase transition	
410	60.7 ± 3.0	759	262.8 ± 8.2
467	79.4 ± 1.7	788	271.0 ± 8.1
530	111.3 ± 0.4	821	287.7 ± 4.7
607	141.1 ± 4.8	839	295.3 ± 2.2
682	177.8 ± 4.1	888	317.1 ± 7.8
747	204.2 ± 0.7		
$Cr_{1.9}Mo_6S_{7.8}$			
298	0	699	192.5 ± 6.1
435	70.2 ± 4.0	759	210.5 ± 6.9
511	104.4 ± 5.0	788	231.4 ± 1.1
580	130.5 ± 5.0	839	249.0 ± 2.7
641	162.4 ± 0.4	896	279.6 ± 3.2
$Cr_{1.9}Mo_6S_{7.9}$			
298	0	699	197.3 ± 5.4
435	72.0 ± 4.0	759	220.9 ± 8.9
511	106.5 ± 5.1	788	235.9 ± 7.7
580	139.6 ± 3.2	839	257.9 ± 5.8
641	167.7 ± 3.2	896	287.2 ± 2.4
$Cr_{2.0}Mo_6S_{8.0}$			
298	0	682	187.8 ± 1.7
410	62.0 ± 1.5	747	221.4 ± 7.0
467	82.3 ± 1.1	821	263.7 ± 3.8
530	115.6 ± 0.9	888	302.0 ± 13.9
607	152.3 ± 2.9		

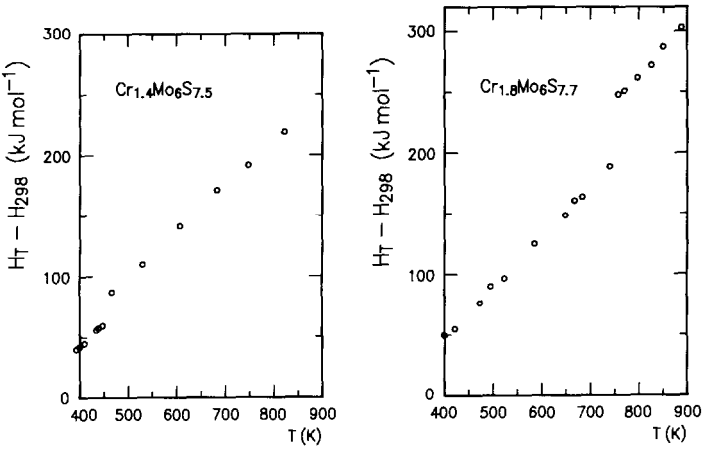

Fig. 5. Dependence of enthalpy increment on temperature for (a) $Cr_{1.4}Mo_6S_{7.5}$ and (b) $Cr_{1.8}Mo_6S_{7.7}$.

with increasing chromium composition. In the rhombohedral structure, Cr atoms occupy two different lattice sites, each representing six symmetry-equivalent point positions (A site and B site). On the other hand, in the triclinic room-temperature modification, they occupy only one lattice site, which represents two symmetry-equivalent point positions (A site) [9]. Thus, the Cr atoms are ordered and form pairs in the triclinic cell. Therefore, the triclinic modification becomes more stable structurally when the chromium composition approaches 2.0.

TABLE 3

Results of drop calorimetry for $Cr_xMo_6S_{8-y}$

Composition of sample, $x, 8-y$	Temperature of phase transition, T_L (K)	ΔH_t (kJ mol^{-1})	ΔS_t (J K^{-1} mol^{-1})	C_p (below T_L) (kJ K^{-1} mol^{-1})	C_p (above T_L) (kJ K^{-1} mol^{-1})
1.4, 7.5	458	21.0	45.9	0.364	0.373
1.4, 7.6	531	32.8	61.8	0.368	0.384
1.5, 7.6	611	43.8	71.7	0.383	0.376
1.5, 7.7	654	41.2	63.0	0.393	0.407
1.6, 7.6	627	47.9	76.4	0.394	0.394
1.6, 7.7	663	46.9	70.7	0.404	0.405
1.7, 7.7	736	50.2	68.2	0.414	0.416
1.8, 7.7	749	50.6	67.6	0.414	0.419
1.8, 7.8	753	51.6	68.5	0.434	0.431
1.9, 7.8				0.452	
1.9, 7.9				0.464	
2.0, 8.0				0.504	

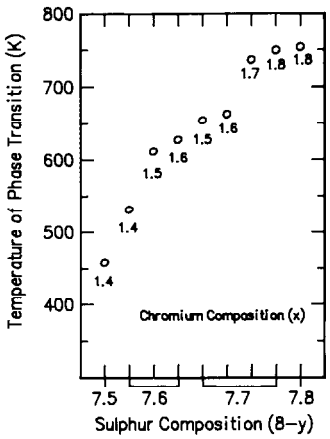

Fig. 6. Relation between the temperature of phase transition and the composition of chromium and sulphur.

Enthalpy of phase transition

Figure 7 shows the chromium composition dependence of the enthalpy of phase transition. This dependence is similar to that for the temperatures of the phase transition. The enthalpy of phase transition increased with increasing chromium composition. However, the increment of the enthalpy of phase transition between chromium compositions 1.4 and 1.6 at a constant sulphur composition of 7.6, was apparently greater than that between Cr compositions 1.5 and 1.7 at a constant sulphur composition of 7.7. It is appropriate to consider that this phenomenon results from the difference in energy states between the A site and B site in the rhombohe-

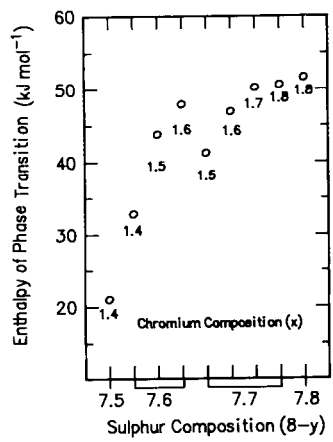

Fig. 7. Relation between the enthalpy of phase transition and the composition of chromium and sulphur.

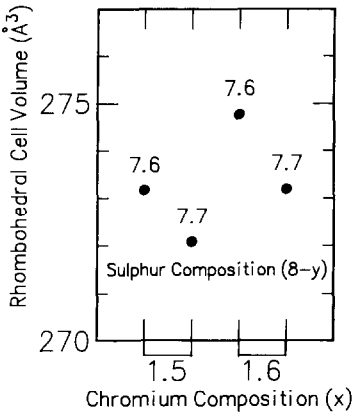

Fig. 8. Dependence of the triclinic and rhombohedral cell volume on compositions.

dral modification (high-temperature phase). In general, the A site is known to be more stable than the B site [10]. That is to say, because chromium atoms begin to occupy the B site in the rhombohedral phase after the transition from chromium composition 1.5 at constant sulphur composition 7.6, the increment in the enthalpy of phase transition was greater than those at a constant sulphur composition of 7.7. The Cr composition dependence of the cell volume of CMS in the rhombohedral phase also supports this view. Figure 8 shows the results for the cell volume evaluated from lattice parameters. It can be seen that the rhombohedral cell volumes with S composition 7.6 are apparently larger than those with S composition 7.7, with chromium compositions 1.5 and 1.6, respectively. We consider that the occupation of the B site by Cr atoms after the transition causes an increase in the unit cell volume in the rhombohedral modification [11].

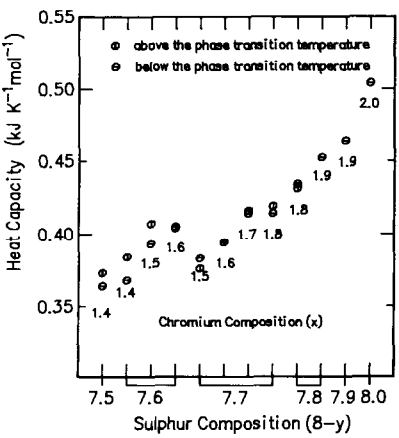

Fig. 9. Relation between the heat capacity and amounts of chromium and sulphur.

An attempt was made to estimate the difference in energies between the A site and B site of chromium in the rhombohedral modification. The differences in the increment in the enthalpy of phase transition between compositions from $Cr_{1.4}Mo_6S_{7.6}$ to $Cr_{1.6}Mo_6S_{7.6}$ and those from $Cr_{1.5}Mo_6S_{7.7}$ to $Cr_{1.7}Mo_6S_{7.7}$ are related to the energy difference between the A site and B site chromium atoms (per 0.2 moles) in the rhombohedral modification. From the above consideration, we estimate the difference in energy between the A site and B site chromium to be about 31 kJ mol^{-1}.

Heat capacity

The dependence of the heat capacities on composition is shown in Fig. 9. According to the results, the heat capacities of CMS increase with increasing chromium and sulphur contents.

REFERENCES

1 M. Marezio, P.D. Derneier, J.P. Remeika, E. Corenzwit and B.T. Matthias, Mater. Res. Bull., 8 (1983) 657.
2 Y.S. Yao, R.P. Guirtin, D.G. Hinks, J. Jorgensen and D.W. Caponell, Phys. Rev. B, 37 (1988) 5032.
3 K. Yvon, A. Paoli, R. Flukiger and D. Grandjean, Acta Crystallogr. Sect. B, 33 (1977) 3066.
4 R. Baillif, K. Yvon, R. Flukiger and J. Muller, J. Low Temp. Phys., 31 (1979) 231.
5 K. Yvon, R. Chevrel and M. Sergent, Acta Crystallogr. Sect. B, 36 (1980) 685.
6 M. Nishio, N. Kuwata, H. Hinode, M. Wakihara and M. Taniguchi, Thermochim. Acta, 88 (1985) 101.
7 N. Kuwata, M. Nishio, H. Hinode and M. Wakihara, Thermochim. Acta, 109 (1986) 181.
8 K.K. Kelley, Bulletin 584, US Bureau of Mines, 1960.
9 K. Yvon, R. Baillif and R. Flukiger, Acta Crystallogr. Sect. B, 35 (1979) 2859.
10 G.J. Dudley, K.Y. Cheung and B.C.H. Steele, J. Solid State Chem., 32 (1980) 259.
11 J. Mizusaki, S.Y. Han, K. Fueki and K. Kitazawa, Solid State Ionics, 11 (1984) 293.